Current Environmental Health Reports (2024) 11:443–451
https://doi.org/10.1007/s40572-024-00450-x

REVIEW

Portable x-ray fluorescence for bone lead measurement: Current approaches and future directions

Aaron J. Specht[1,2] · Christian Hoover[3,4] · Thomas Grier[1]

Accepted: 15 May 2024 / Published online: 22 May 2024

Abstract

Purpose of Review Legacy lead exposures persist as a widespread problem. Blood lead is traditionally used for lead exposure surveillance; however, bone lead proves to be a cheaper, more accessible, and more revealing tool for surveillance that can be measured using portable x-ray fluorescence techniques. We outline how this approach excels for bone lead measurements.

Recent Findings Portable XRF offers quick, non-invasive in vivo quantification of bone lead. Compared to traditional KXRF systems, pXRF is limited to cortical bone but allows for quicker and similar results. Current methodologies of lead exposure need re-evaluation as lead-related disease burden and trends are dependent on both cumulative and acute impacts.

Summary We examined the evolution of XRF techniques for measuring bone lead, comparing current methods with previous ones. We assessed their accuracy, identified limitations, and discussed potential advances in future techniques. Legacy lead exposures call for a revitalization of lead surveillance methods, and pXRF measurement of bone lead offers such a solution.

Keywords Heavy Metals · X-ray fluorescence · In vivo quantification · Portable · Surveillance

Introduction

Lead is a significant driver of disease and mortality worldwide, with studies indicating any exposures has vast impacts on mortality, neurodevelopment, and cardiovascular health [1–4]. Traditionally, lead surveillance is done using blood lead, but these measurements in the context of our public health standards only reflect acute exposures [5]. Blood lead in adults has a half-life of about 30 days with studies indicating the youngest children have a blood lead half-life of a week [6–9]. Lead acts in the body by mimicking calcium and accumulates in bones [6]. Bone, which turns over slowly in the body, serves as a long-term marker of lead exposure with a half-life of 20–30 years [6, 10, 11]. Even in young children, where bone turnover is very fast, bone lead can serve as a biomarker for years of exposure [9, 11]. This is often discussed in studies of serial lead measurements, many indicating peak blood lead or cumulative blood lead indices, indicated with bone lead, better reflects neurodevelopment over either average or singular blood lead levels [1, 3]. While bone lead is known to be the better biomarker of exposure to lead, the use of this valuable technology has historically been limited by the difficulties of the technology itself.

Traditionally, bone lead is measured using x-ray fluorescence (XRF). This measures the bone non-invasively in vivo. By far the most successful XRF measurement systems for measuring bone lead focuses on utilizing the K-shell of lead, commonly referred to as KXRF measurements [6, 12, 13]. The KXRF systems uses a cadmium-109 radioisotope source for measurement of lead over the mid-tibia. Although this system produces reliable results, and iterations have improved detection capabilities, it is rarely used due to many significant disadvantages [12, 13].

Chief among the disadvantages for the KXRF system was the use of a radioisotope source. The use of the radioisotope source was a major hurdle to most institutions requiring significant regulatory intervention prior

This article is part of the Topical Collection on *Metals and Health*

✉ Aaron J. Specht
aspecht@purdue.edu

1 School of Health Sciences, Purdue University, 550 Stadium Mall Drive, West Lafayette, IN 47907, USA

2 Harvard T.H. Chan School of Public Health, Boston, MA 02115, USA

3 Department of Epidemiology, Brown School of Public Health, Providence, RI, USA

4 Harvard Injury Control Research Center, Harvard T.H. Chan School of Public Health, Boston, MA, USA

to receiving the source. Within the United States, this required amendment of an institutions' broad scope license with the nuclear regulatory commission, presenting significant burden and disincentivizing institutions. Further issues abound: 1) global trade restrictions make it almost impossible in to refresh cadmium sources for these systems, a biennial requirement; 2) the KXRF instrument operates using germanium detections, requiring liquid nitrogen cooling to function; and 3) the dewar, associated with cooling, makes the instrument more cumbersome and is far more costly given its association with liquid nitrogen (a material requirement of refreshing the dewar). Perhaps most critically, the KXRF requires a 30-min measurement time. This creates immediate issues with scalability for institutions and convenience for patients and participants; when only 16 individuals can be measured in an 8-h time period, surveillance becomes almost impossible.

Bone lead measurements have generally provided stronger associations with health outcomes when compared to blood measures of exposure. However, the KXRF has substantial issues, restricting its utility to only a few extremely well-funded institutions worldwide. As such, there is a pressing need for a device capable of measuring bone lead in a portable, cost-effective, and convenient method. This criterion appears to be well met with the novel portable x-ray fluorescence device, or pXRF.

The pXRF device was first validated in 2016 and leverages a lower energy technology [9, 14, 15]. X-rays from the device knock out inner shell electrons of an atom. Because the atom wants to be in a stable configuration, an electron from a higher shell will deexcite to fill the created space. In this deexcitation process, the energy is released as a photon known as a characteristic X-ray. Figure 1 highlights the physics behind this phenomenon. The nomenclature of L-shell XRF as well as pXRF refer to utilizing the X-rays generate from electrons falling from higher orbitals into the L-shell of the atom. Similarly, KXRF refers to using the X-rays generated from electrons from higher orbitals falling into the innermost shell of the atom, the K-shell.

This technology was previously attempted for utilization in bone lead measurement but presented problems in correcting for soft-tissue thickness [16, 17]. However, while research has since sufficiently demonstrated the utility and validity of the research of the novel pXRF utility, there have been no studies to date that review this body of literature. In this article, we will summarize previous literature, the standards for technical specifications and analysis, and utility of this technique for future studies to provide an authoritative source on the pXRF for public health and government entities.

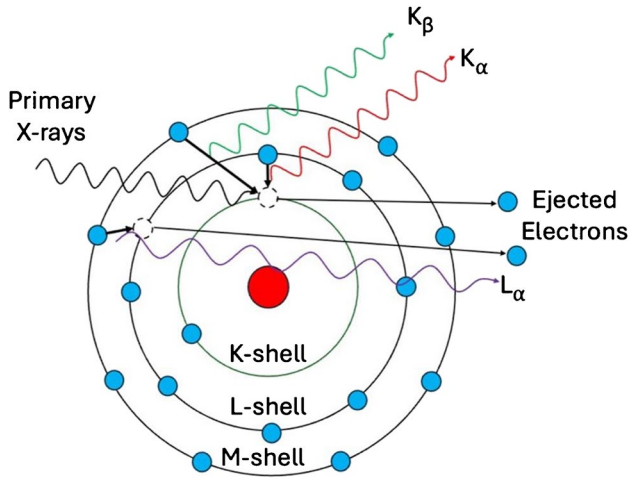

Fig. 1 Physics behind X-ray fluorescence. K-shell XRF refers to the technique utilizing X-rays generated with deexcitation to the K-shell. L-shell or pXRF refer to utilizing the ones generated with deexcitation to the L-shell

Methods

Comparison between KXRF and pXRF

KXRF and pXRF have been compared in a number of studies to this point. In a population of environmentally exposed individuals, it was found that KXRF and pXRF had a correlation coefficient of 0.48 for all participants [18]. Restricting to only individuals with uncertainty lower than 10 μg/g from both KXRF and pXRF gave a correlation coefficient of 0.83 in the study [18]. Previous comparisons involved both KXRF and inductively coupled plasma mass spectrometry in comparison to pXRF with correlations ranging from 0.88 to 0.94 [19, 20]. Finally, a study using a lower measurement time in children compared KXRF and pXRF giving a correlation coefficient in the full population of 0.43 and demonstrating significant differences between lead poisoned and control populations using the pXRF [8, 9].

Current Technology for use with L-shell XRF for Bone Lead Measurements

The current methodology utilizes a pXRF from Thermo Fisher (Thermo Fisher Niton XL3t GOLDD+, Thermo Fisher Billerica, MA) [15, 18]. Although this is the XRF utilized in the project, we have found any pXRF with comparable geometry and radiation detectors would suffice for equivalent measurements given proper calibration and dosimetry. The system utilizes a standard 50 kV x-ray

tube with a silver anode operated at 2-W output (40 uA). A molybdenum anode could be used but corresponding scattering peaks lower the initial energy from the characteristic x-rays closer to that of elemental peaks of interest. Silver at 22 keV, after undergoing Compton scattering in which its emitted X-ray loses some energy after interacting with an electron, produces a secondary peak at 20 keV [9, 15]. Similarly, molybdenum, initially at 17.5 keV, give rise to Compton scattered x-rays at about 16.5 keV for an approximate 160° backscatter geometry.

The backscatter geometry is key to the XRF measurements in bone. Any high-density material will produce surface level interactions and signals within the first few millimeters [21]. A 90° geometry or non-backscatter geometry for low energy x-rays drastically decreases signal production through increased skin thickness for attenuation of outgoing signal. In addition, the isotropic production of signal from XRF will drop significantly with added distance. A 90° geometry adds significant distance when considering a true in vivo measurement. Even the addition of a few millimeters will lead to a drop in signal of almost 50% [15]. In a study in 2014, we presented data indicating air gaps were causing a significant signal decrease based on this same reasoning [15]. A significant drop in signal will lead to dramatic differences in detection capabilities for the overall system. Finally, the system utilizes a filter of the x-ray beam using the same high-Z material of the anode. While the Thermo device uses a silver filter and anode, any similar filtration combination that preferentially reduces unnecessary low-energy background and increases high-energy x-rays capable of producing signals should allow for an optimized measurement. The filter size is dependent mostly on the radiation detector chosen.

The radiation detector most typical of XRF for L-shell techniques is a silicon drift detector. Current detector systems have a wide range of capabilities. Some can measure ~ 300 k counts per second utilizing high-throughput electronics. These systems usually rely on the initial dead time being closer to 50%, utilizing an electronic counting technique to include signals ordinarily left out of final analyses. Most XRF's, including the Thermo XRF, still utilize a standard counting method with count rates of ~ 50-60 k count per second and achieving detection limits capable of identifying most environmental exposures to lead from bone. The application of new radiation detectors into pXRF will allow for a reduction of the bone lead detection limit by a factor of ~ 2–3.

Correction for Overlying Tissue

A major drawback of utilizing pXRF technology is the reliance on correction factors to account for overlying tissue thickness. Overlying tissue thickness has two main roles in the bone measurements: 1) as an additional attenuator for the exiting lead signal from the bone towards the detector; and 2) as a perpetuator of an inverse square drop off of signal by increasing the distance between the sample, we wish to primarily measure, namely bone, and the detector. These two factors combine to drop the signal with increasing tissue thickness over bone, which can be seen clearly in Fig. 2 indicating the decrease in 100 µg/g lead phantom signal with increasing Lucite thickness which is meant to act similarly to tissue.

Current XRF approaches for measuring bone lead using L-shell XRF utilize a normalization factor from Compton scattering for calibration, which chiefly is used to account for the effect of overlying tissue thickness on the measurement. Specifically, the silver anode Compton scattering peak was identified as a good predictor of soft tissue thickness [14, 15]. In addition, the Compton scattering peak has been shown to be reflective of other potential factors in the measurement of bone lead, such as bone geometry and

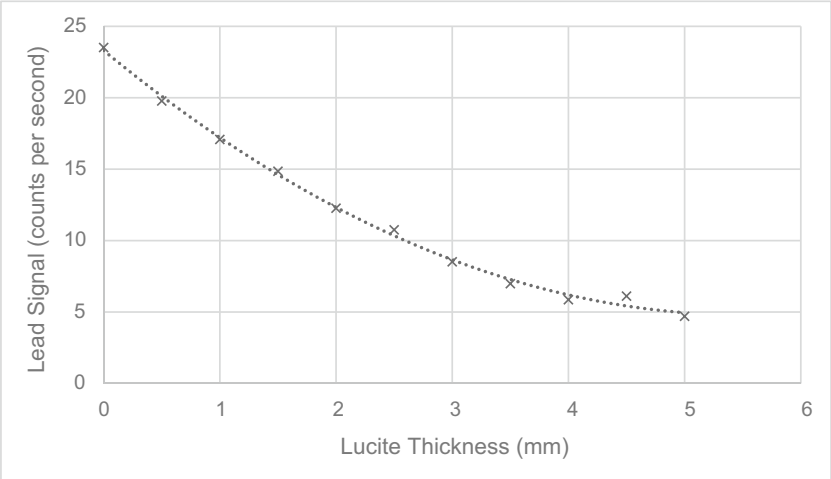

Fig. 2 Lead signal counts with increasing tissue thickness

composition [9, 21]. In the initial study from Nie et al., the anode Compton scattering peak had good predictability of soft tissue thickness but was not a perfect predictor, which was similarly found for increasing phantoms of soft tissue utilized in other studies [9, 14, 15]. This observation was a direct result of the Compton scattering that served as a normalization factor for other geometry and composition anomalies within in vivo measurements. This was confirmed in further studies utilizing this normalization approach for varying mass of in samples and when doing comparisons of bone with and without soft tissue measured via pXRF [19, 22, 23]. The normalization differences are also evident when examining the resultant differences from calibrating with goat bone versus plaster-of-Paris phantoms [15]. Furthermore, the Compton scattering peak identified could be fit using a traditional gaussian. In this case, the peak itself is heavily skewed due to the surrounding x-ray anode interactions but is sufficient to utilize a summation of channel intensities from within plus or minus 0.5 keV from the Compton scattering peak at 20.5 keV.

The Compton scattering normalization was built into the calibration alongside the 100 µg/g phantom for measurements of signal decreases with relative increasing Lucite thickness [15, 18, 19]. The calibration for concentration was found to act linearly with increasing counts proportional to concentration, but a polynomial fit was best used for decreasing counts based on increased Compton scattering from Lucite [15, 18]. This interaction would normally be an exponential decay, but experimental measures before and after soft tissue removal confirmed that the polynomial fit worked best [19]. Given the linear relationship with counts, the primary calibration requires a high concentration plaster-of-Paris lead standards and tissue equivalent plastic such as Lucite of varying thickness from 1 to 5 mm. This range of Lucite was shown to give enough predictability to the calibration fit without introducing geometry errors [18, 19]. The beam exits the x-ray aperture at about a 10° angle to the right angle norm. Thus, may be difficult to present a 1 cm^2 phantom perfectly within the beam structure at more than 5 mm of soft tissue phantom.

Fitting of the XRF Spectra

Identification of the lead signal was tested in multiple ways using the 10.5 and 12.6 keV lead L-shell peaks [15]. The L-alpha peak at 10.5 keV is a frequently utilized peak in XRF due to its higher yield compared to the corresponding L-beta peak at 12.6 keV. However, the alpha peak demonstrated some severe difficulties in disentangling the interactions with zinc (K-shell), mercury, and arsenic (K-shell) peaks in the same energy region [9, 15]. Alternatively, the beta peak is far removed from elements typically seen in biological material. Thus, for bone lead the beta peak is primarily used for quantification [9, 18]. The fitting method utilized was a standard gaussian fit with an exponential background to identify net counts of the beta peak for lead [9]. This equation

$$a * \exp\left[-0.5\left(\frac{x-b}{c}\right)^2\right] + d * \exp\left[x * f\right],$$

where x is the energy corresponding with the energy spectra, a is the gaussian height, b is the gaussian location, c is the gaussian width, d is the background intensity, and f corresponds with the exponential decay of background intensity. We restricted fitting to within 12.56 to 12.66 keV for peak location, and the radiation detector properties dictate the width of the peak c to be approximately 0.05 keV, but we gave a range of 0.01 to 0.1. For the fitting to resolve, the width and peak location need to have flexibility, as the background levels can change both parameters. The minimum peak width can typically be set lower than the radiation detector gain but should be higher than zero to avoid. This balance avoids false negatives and false positives in the fitting method based on noise in the spectra. An example of a fitted peak is shown in Fig. 3.

Units of Bone Lead Measurement

The units for measurement were identified to be µg/g bone mineral, which would be equivalent and comparable to previous studies utilizing KXRF [20]. Previous studies using inductively coupled plasma mass spectrometry (ICPMS), KXRF and pXRF confirmed the units for measurements and conversion factor from the initial calibration in dry bone [20]. Our previous work highlighted measurements using the standard calibration with plaster-of-Paris doped

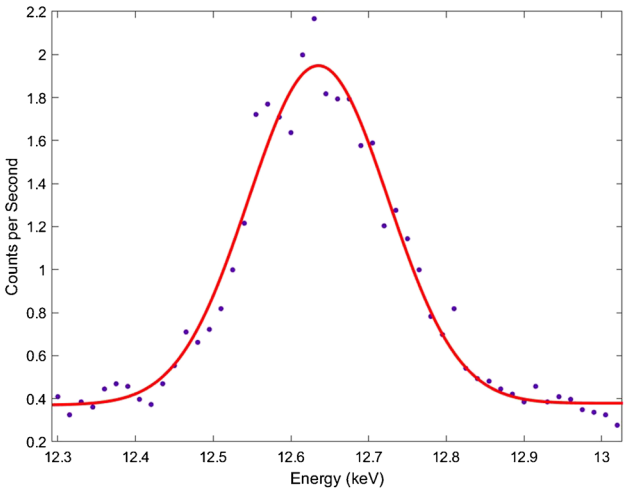

Fig. 3 Example fitted lead L-beta peak from pXRF measurements

bone phantoms to calculate in vivo bone lead from pXRF and KXRF, along with lab bone samples measured using pXRF, KXRF, and ICPMS. In comparison with all of this data, there was found to be a conversion factor of approximately 1.5 from the standard dry bone pXRF calibration for in vivo bone lead measurement in order to change the units to microgram per gram bone mineral content [15, 18, 21].

Uncertainty Measures and Statistical Treatment

Initial studies attempted to take into account the added uncertainty of normalizing for soft tissue thickness, but consistently came up with an overestimation of uncertainty measures [14, 15, 21]. The final method used a simple error propagation from standard counting statistics based entirely on the peak statistics from the lead L-beta line [9, 18, 24]. This error propagation method can be calculated using the equation

$$\sigma = \frac{\sqrt{\text{BKG}}}{\text{Net}},$$

where σ is the uncertainty as one standard deviation, BKG is the background counts under the lead L-beta peak, and Net is the net counts from the lead L-beta peak.

Similarly, to previous KXRF measures, the pXRF produces a point-estimate of bone lead. This means that if the actual results are close to zero, the estimate can be negative. Typically, other spectroscopy techniques will incorrectly identify these are below a detection limit and cut them off at 0 – biasing the data artificially. Studies using KXRF measurements identify that this unnecessarily biases the measurement analyses for the aggregate data [25]. Thus, the data should be analyzed as is when utilizing negative results to account for instrumental inaccuracies within the calculation. However, many analyses have additional considerations since exposure data is quite often skewed and non-normal [26]. For these concerns, it is generally best practice to demonstrate either a trend across quartiles of the data or use a transformation. However, it is still appropriate to give non-transformed results and, in some cases, may give valuable information. Generally, reporting all analyses and potential changes under transformation gives the most accurate data for the broader scientific community.

Finally, it has been shown that uncertainty weighting for analyses can be used if the uncertainties are high enough to warrant it [18, 21, 27]. This technique utilizes an inverse squared weight generated by the uncertainty as a normalization dictated by $Weight = \frac{1}{U^2}$, where U is the uncertainty given by the counting statistics and spectral fitting. Depending on the statistical approach these weights may or may not need to be normalized to 1 within the aggregate data. However, this was shown to be unnecessary if the uncertainties of the underlying data are low enough to be ignored, such as with the 5-min bone lead measurements in Zhang et al. 2021 [18]. Generally, uncertainty is considered low, if either the uncertainty itself is less than the measurement result or the uncertainty is less than 10 µg/g.

Measurement Time

The time for each measurement has changed iteratively along with the identification of the optimized methodology [9, 15, 18–20]. Initially two-minutes was thought to produce counting statistics capable of environmental exposures, but this inadequately represented the complexity of in vivo measurements [9]. While a 3-min measurement is now considered optimal, for populations with more soft tissue thickness and correspondingly greater uncertainties this was shown to be too little [18]. In more recent studies, it is suggested that this be based primarily off live-time of the detector with a range of measurements from 3 to 5 min depending on the uncertainties produced during measurements [18]. As mentioned below, dosimetry dictates below a ten-minute measurement to be safe, but experimentally a 5-min measurement is more than sufficient to minimize the uncertainty based on soft tissue thickness [18, 28]. In practice, the live time of the detector, which is displayed on-screen during measurements, is the best indicator of relative precision of the measurement. Thus, rather than using an arbitrary time, we generally use a live time to match with the level of statistical certainty necessary for measurements, which will vary the real time based on an individual's characteristics but give a standard statistical certainty. For example, an individual with a larger bone and thin soft tissue could have a measurement time of less than 3-min, but an individual with a small bone and higher soft tissue, giving less overall useful counts for our measurement, could have a measurement time of greater than 3-min.

Radiation Dose from pXRF Measurements

A comprehensive dosimetry assessment was done as part of a previous study utilizing the pXRF [28]. This study was completed using a standard 2 W x-ray tube with 50 kV and 40 microamps x-ray tube. Using optically stimulated luminescent dosimeters the highest dose we could achieve with a 3-min measurement to the ~ 0.2 cm^2 of the OSLD was 103.7 mSv, which could serve as a check on any new XRF sources to ensure operating within safe limits. In said study, a Monte Carlo simulation was believed to give the most accurate results for dosimetry purposes by perfectly evaluating the voxels that would have received any exposure. Using this simulation, we found that a conservative estimate for total body effective dose was 3.4 µSv with a 3-min measurement. The normalized skin and bone doses were averaged only over the leg of individuals, and when

considering the total bone and skin area, the total body effective dose would diminish by an additional factor of > 10 to approximately 0.34 μSv (0.034 millirem). For reference, this dose from the pXRF system is comparable to that of the KXRF system each system for adults or children having a dose of < 5 μSv [9].

Although radiation doses from such a small beam is an anomaly to many health physics practitioners, it is akin to the treatment of 'hot particles', which were used in the establishment of skin dose limits for occupational health [29, 30]. The current deterministic risk from a 3–5-min measurement is 100–200 times less than any dose necessary to cause any potential effect [28]. Thus, the radiation dose from a pXRF measurement is nominal – representing incalculable risk to an individual, in light of the negligible total body radiation dose contributing to potential risk of cancers. For comparison, more radiation is achieved from natural background or cosmic sources in a given 12-h period than is achieved from a single pXRF measurement. The radiation dose from a single pXRF measurements is 1/30th of typical chest x-rays and, depending on dental x-ray parameters, can be less than 1/3rd of a dental x-ray. The dose is less than one receives from being on an airplane for 3 h.

Discussion

Limitations of PXRF Bone Lead Measurements

There are some limitations to the use of the pXRF in relation to less convenient devices. First and foremost, soft tissue thickness may create issues with precision, although much less so when using longer measurement time based on a recent study of in vivo measurements [18, 19]. In practice, most individuals have a soft tissue thickness that is low enough to be accurately measured for bone lead at the mid-tibia [21]. It also seems that additional uncertainty generated by soft tissue is fairly meaningless utilizing consistent live times for adequate statistics [18]. Utilizing a cut-off for uncertainty is likely still the best practice for dealing with any individual level data, but aggregate data should be treated as-is with point-estimates.

Comparison to Radioisotope based KXRF Bone Lead Measurements

Previous bone lead measurements using cadmium-109 based KXRF would give two main advantages over currently utilized pXRF technology. First, the KXRF energy allows for investigations identifying cortical and trabecular bone measurements, whereas pXRF L-shell measurements can only measure cortical bone. Studies of the pXRF measurement of bone found that it is limited to measurements of cortical bone because the energies of these X-rays do not allow for penetration to the trabecular bone to get a signal [21, 31]. Even in cases of bones that are primarily trabecular, the cortical bone appears to be the only site measured [21, 31]. This is in contrast to KXRF measures which utilized both primarily cortical, at the mid-tibia, and primarily trabecular, at the patella, bone sites to differentiate between readily accessible lead in bone and long-term storage of lead in bone [6, 32]. Cortical bone, measured at the mid-tibia, does give the best estimate for long-term cumulative exposure to lead, leading to decades of exposure time [6, 10]. Secondly, uncertainty measures have the potential of varying based on individuals. This has not been confirmed as a problem in a major cohort study, but, if it is shown to be problematic, the solution would be to routinely perform uncertainty weighted analyses. Previous KXRF measures did not completely overcome this issue, as the uncertainty would still change with radioisotope decay over the course of data collection. Utilizing a cut-off for uncertainty is often incorporated in KXRF measurements with an uncertainty above 10 or 15 μg/g recommended to be removed [32].

Previous Studies of L-shell XRF

Previous utilization of the L-shell technique for measurement of bone lead was done first in the early 80's [33]. The technique was tested in children utilizing a 15-min measurement time [17]. This study accounted for skin thickness by utilizing a correction alongside ultrasound measurements. The system utilized as part of this study was found to be valid for identification of bone lead, but the skin thickness correction proved difficult and drastically impacted the detection capabilities. A key factor for the detection differences in this system, versus the currently utilized pXRF technology is the geometry for measurement and radiation detector technology. The 90° geometry made signal-to-noise and detection limits much greater than the currently utilized XRF technique. This basically created a situation in which the variability from background was greater than the signal generated during actual bone lead measurements. Additionally, the soft tissue correction without using spectral results made it impossible to account for other geometry issues experienced during in vivo measurements, such as slight changes in bone geometry which could account for drastic changes in signal and measured lead concentration for L-shell energies.

More recently, Todd et al. utilized the L-shell technique similar to the setup in the early 2000's [16, 34, 35]. The 90° geometry would have reduced difficulties with signal to noise but likely increased skin thickness perturbation of results. Similarly, a tissue correction factor was used in this study, but, unfortunately, would not have accounted for the other confounding variables in the geometry that would

have been included in the anode Compton normalization for pXRF measurements. In these studies, Todd et al. points to the inadequacy of correction based on soft tissue alone, as adipose and soft tissue have differing attenuation factors for the signal [34, 35]. Thus, a normalization based on spectral features creates a much easier methodology when accounting for the myriad variables in measurements.

Future Utilization and Technological Advances for the XRF and Bone Technique

L-shell lead measurements using a pXRF likely are the start of a revitalization of exposure assessment for other elements known to accumulate in bone. Many heavy metals like arsenic and uranium are bone seeking elements due to the properties similar to calcium and could be measured with this system [24, 36]. Nutritionally essential elements oftentimes are bone-seeking and involved in body homeostasis, such as copper and zinc [37, 38]. The low energies of the pXRF would warrant caution when looking at elements such as manganese with characteristic energies of 5.9 keV that would be absorbed quickly in overlying tissue, but the elements with slightly higher energies or that accumulate in bone at higher concentrations could easily be quantified. Figure 3 illustrates this point effectively by demonstrating the peaks for nickel, iron, and zinc from an in vivo measurement.

Technological advances in radiation detection allow for drastic increases in signal to noise and counting statistics in terms of XRF measurements. Semi-monoenergetic peaks can be obtained using optical properties and are utilized in different XRF devices to reduce the background otherwise created from bremsstrahlung to almost null [39–41]. In this instance, semi-monoenergetic refers to X-ray peaks that do not consist purely of a single energy, but are close to being so (small range of energies around the peak). This can give a signal to noise ratio that is unprecedented in current XRF techniques. However, optics can severely limit the beam flux from the initial x-rays – impacting the overall signal production as well. More studies on how these two beam types compare are needed.

High throughput detector electronics have been implemented in benchtop XRF but underutilized in the pXRF counterparts [42]. This would drastically decrease detection limits for most elements, as the in vivo measurements already have dead times within the optimal 50% range for these electronics to be fully utilized and may decrease detection limits by a factor of 2. Similarly, the small form factor of these detectors would easily allow for a multi-detector setup as has been done with previous KXRF techniques [12, 43]. Relatedly, high energy x-ray tubes capable of producing energies above 88 keV can be utilized to measure the K-shell of lead without many of the limitations of traditional KXRF technology [21, 44]. Additionally, this would allow for the potential of measuring both cortical and trabecular bone sites, which is a major current limitation, for comparisons in epidemiological studies; many previous studies indicated differences between the two biomarkers in terms of health outcomes [32, 45–48].

A novel micro-XRF grazing approach, utilizing the L-shell XRF energies for bone lead measurement, is being tested [49, 50]. Currently the detection limits are similar to the pXRF approach with a much more complex geometry. If the geometry for in vivo measurements could be replicated without additional time needed for setup and verification, the device could prove very useful for future bone metal detection. However, the device in its current state uses a longer measurement time than pXRF approaches to achieve similar results [49].

Conclusions

The pXRF is a much more widely available method for measurement of cumulative lifetime lead exposure and should be leveraged in more studies and surveillance programs. It is more convenient for participants and patients through a reduced scan time(3–10 min, depending on individual characteristics, versus 30 min), is much more affordable, can be transported easily given its handheld form factor, and may likely prove even more useful in future iterations and when examining other metal exposures. In consideration of lead exposure, it is clear that current methodologies, especially for assessment in children, need re-evaluation as the blood lead levels and half-lives become more of a limitation to ongoing studies and population surveillance [8, 9]. This presents a critical gap in public health and emphasizes the requirement of more accurate testing. Despite efforts to reduce lead exposure, a significant number of children have elevated levels. Hautptman et al. postulate as many as half of all children in the United States display elevated blood lead levels with Lanphear et al. demonstrating increased mortality from the adults still suffering from the lingering impacts of legacy lead exposures [1, 2, 51–53]. This number may continue to remain high given the limitations inherent to blood lead testing and the limited number of population-based studies with measures of bone lead; a limitation rectifiable with more advanced and comprehensive exposure assessments, such as the pXRF – already proven to work well in determining exposure levels in children [8].

When cumulative lead exposure is poorly measured, health-related outcomes in later life may be attributed to other causes. For example, a study published in 2023 posits that estimations of lead-induced cardiovascular disease related to mortality are almost always due to hypertension, but that lead exposure has myriad effects that contribute

to cardiovascular disease, of which a primary signal is not hypertension (e.g., hardening of the arteries). The authors estimated that the actual global burden of lead exposure is closer to 5.5 million (six times higher than previous estimates) [54]. While we have indeed made great progress in lead surveillance, blood alone is insufficient, providing a limited scope and requiring substantial resources in order to determine consistent low-levels [5, 55]. This poses a major risk to children and adults, especially when research has shown the increased risk of lead exposure more broadly, and from sources that have not previously been investigated [1, 2, 56, 57]. Integrating the pXRF device in surveillance and monitoring is essential, given its considerably strengths relative to the limitations of blood lead testing. States and policy makers should consider the pXRF device in future programs targeting lead remediation, prevention, and monitoring.

Acknowledgements This manuscript was partly funded by a K01 award from NIOSH grant number K01OH012528 and DoD CRMP 12971061. At the time of this writing, Dr. Aaron Specht has a provisional patent proposal at the USPTO (patent number 63/420,136) based on some information provided herein.

Author contributions Aaron J Specht Writing, Conceptualization, Methodology, Reviewing, Editing. Christian Hoover Writing, Methodology, Reviewing, Editing. Thomas Grier Writing, Methodology, Reviewing, Editing.

Declarations

Conflicts of Interest Dr. Aaron Specht has a provisional patent proposal at the USPTO based on some information provided herein.

Human and Animal Rights and Informed Consent This article does not contain any studies with human or animal subjects performed by any of the authors.

References

1. Lanphear BP, Hornung R, Khoury J, Yolton K, Baghurst P, Bellinger DC, et al. Low-level environmental lead exposure and children's intellectual function: an international pooled analysis. Env Health Perspect. 2005;113(7):894–9.
2. Lanphear BP, Rauch S, Auinger P, Allen RW, Hornung RW. Low-level lead exposure and mortality in US adults: a population-based cohort study. Lancet Public Health. 2018;3(4):e177–84.
3. Canfield RL, Henderson CR, Cory-Slechta DA, Cox C, Jusko TA, Lanphear BP. Intellectual impairment in children with blood lead concentrations below 10 μg per deciliter. N Engl J Med. 2003;348(16):26.
4. Lamas GA, Bhatnagar A, Jones MR, Mann KK, Nasir K, Tellez-Plaza M, et al. Contaminant Metals as Cardiovascular Risk Factors: A Scientific Statement From the American Heart Association. J Am Heart Assoc. 2023;12(13): e029852.
5. Rabinowitz MB. Toxicokinetics of bone lead. Env Health Perspect. 1991;91:4.
6. Hu H, Rabinowitz M, Smith D. Bone lead as a biological marker in epidemiologic studies of chronic toxicity: conceptual paradigms. Environ Health Perspect. 1998;106(1):1–8.
7. Rabinowitz MB. Bone lead as a biological marker in epidemiologic studies of chronic toxicity: conceptual paradigms. Env Health Perspect. 1998;106:8.
8. Specht AJ, Weisskopf M, Nie LH. Childhood lead biokinetics and associations with age among a group of lead-poisoned children in China. J Expo Sci Environ Epidemiol [Internet]. 2018 Apr 30; Available from: https://doi.org/10.1038/s41370-018-0036-y.
9. Specht AJ, Lin Y, Weisskopf M, Yan C, Hu H, Xu J, et al. XRF-measured bone lead (Pb) as a biomarker for Pb exposure and toxicity among children diagnosed with Pb poisoning. Biomarkers. 2016;21(4):347–52.
10. McNeill FE, Fisher M, Chettle DR, Inskip M, Healey N, Bray R, et al. The decrease in population bone lead levels in Canada between 1993 and 2010 as assessed by in vivo XRF. Physiol Meas. 2017;39(1): 015005.
11 ICRP. Publication 70, Basic anatomical and physiological data for use in radiological protection - the skeleton. Ann ICRP. 1995;25(2):1–80.
12. Nie H. Studies in bone lead: A new cadmium-109 XRF measurement system. Modeling bone lead metabolism. Interpreting low concentration data [Internet] [Thesis (Ph D)]. McMaster University (Canada), 2005.; 2005. Available from: http://libaccess.mcmaster.ca/login?url=http://wwwlib.umi.com/dissertations/fullcit/NR07922. Accessed 13 Nov 2023.
13. Chettle DR, Scott MC, Somervaille LJ. Lead in bone: sampling and quantitation using K X-rays excited by 109Cd. Env Health Perspect. 1991;91:49–55.
14. Nie H, Sanchez S, Newton K, Grodzins L, Cleveland RO, Weisskopf MG. In vivo quantification of lead in bone with a portable x-ray fluorescence system–methodology and feasibility. Phys Med Biol. 2011;56(3):N39-51.
15. Specht AJ, Weisskopf M, Nie LH. Portable XRF Technology to Quantify Pb in Bone In Vivo. J Biomark. 2014;2014: 398032.
16. Todd AC, Carroll S, Geraghty C, Khan FA, Moshier EL, Tang S, et al. L-shell x-ray fluorescence measurements of lead in bone: accuracy and precision. Phys Med Biol. 2002;47:20.
17. Rosen JF, Markowitz ME, Bijur PE, Jenks ST, Wielopolski L, Kalef-Ezra JA, et al. Sequential measurements of bone lead content by L X-ray fluorescence in CaNa2EDTA-treated lead-toxic children. Env Health Perspect. 1991;93:271–7.
18. Zhang X, Specht AJ, Wells E, Weisskopf MG, Weuve J, Nie LH. Evaluation of a portable XRF device for in vivo quantification of lead in bone among a US population. Sci Total Environ. 2021Jan;20(753): 142351.
19. Specht AJ, Kirchner KE, Weisskopf MG, Pokras MA. Lead exposure biomarkers in the Common Loon. Sci Total Env. 2019;10(647):639–44.
20. Specht AJ, Parish CN, Wallens EK, Watson RT, Nie LH, Weisskopf MG. Feasibility of a portable X-ray fluorescence device for bone lead measurements of condor bones. Sci Total Env. 2018;15(615):398–403.
21. Specht AJ, Dickerson AS, Weisskopf MG. Comparison of bone lead measured via portable x-ray fluorescence across and within bones. Env Res. 2019;172:273–8.
22. Bhatia M, Specht AJ, Ramya V, Sulaiman D, Konda M, Balcom P, et al. Portable X-ray Fluorescence as a Rapid Determination Tool to Detect Parts per Million Levels of Ni, Zn, As, Se, and Pb in Human Toenails: A South India Case Study. Environ Sci Technol. 2021;55(19):13113–21.
23. Specht AJ, Kponee K, Nkpaa KW, Balcom PH, Weuve J, Nie LH, et al. Validation of x-ray fluorescence measurements of metals in toenail clippings against inductively coupled plasma mass spectrometry in a Nigerian population(). Physiol Meas. 2018;39(8): 085007.

24. Specht AJ, Mostafaei F, Lin Y, Xu J, Nie LH. Measurements of Strontium Levels in Human Bone In Vivo Using Portable X-ray Fluorescence (XRF). Appl Spectrosc. 2017;71(8):1962–8.
25. Kim R, Aro A, Rotnitzky A, Amarasiriwardena C, Hu H. K x-ray fluorescence measurements of bone lead concentration: the analysis of low-level data. Phys Med Biol. 1995;40(9):1475–85.
26. Specht AJ, Lin Y, Xu J, Weisskopf M, Nie LH. Bone lead levels in an environmentally exposed elderly population in shanghai. China Sci Total Env. 2018;1(626):96–8.
27. Johnson KM, Specht AJ, Hart JM, Salahuddin S, Erlinger AL, Hacker MR, et al. Lead exposure and association with angiogenic factors and hypertensive disorders of pregnancy. Pregnancy Hypertens. 2020;22:93–8.
28. Specht AJ, Zhang X, Goodman BD, Maher E, Weisskopf MG, Nie LH. A Dosimetry Study of Portable X-ray Fluorescence in Vivo Metal Measurements. Health Phys. 2019;116(5):590–8.
29. Baum JW, Cantea AL, burin DGL, Schaefer CW. Acute skin lesions due to localized "hot particle" radiation exposures. Brookhaven Natl Lab Rep. 1996;BNL-NUREG-62140.
30. Charles MW, Harrison JD. Hot particle dosimetry and radiobiology–past and present. J Radiol Prot Off J Soc Radiol Prot. 2007;27(3A):A97-109.
31. Specht AJ, Steadman DW, Davis M, Bartell SM, Weisskopf MG. Bone lead variability in bone repository skeletal samples measured with portable x-ray fluorescence. Sci Total Environ. 2023;1(880): 163197.
32. Weisskopf MG, Proctor SP, Wright RO, Schwartz J, Spiro A, Sparrow D, et al. Cumulative lead exposure and cognitive performance among elderly men. Epidemiology. 2007;18(1):59–66.
33. Wielopolski L, Rosen JF, Slatkin DN, Vartsky D, Ellis KJ, Cohn SH. Feasibility of noninvasive analysis of lead in the human tibia by soft x-ray fluorescence. Med Phys. 1983;10(2):248–51.
34. Todd AC. L-shell x-ray fluorescence measurements of lead in bone: system development. Phys Med Biol. 2002;47:15.
35. Todd AC. L-shell x-ray fluorescence measurements of lead in bone: theoretical considerations. Phys Med Biol. 2002;47:14.
36. Rodríguez J, Mandalunis PM. A Review of Metal Exposure and Its Effects on Bone Health. J Toxicol. 2018;23(2018):4854152.
37. Rondanelli M, Faliva MA, Infantino V, Gasparri C, Iannello G, Perna S, et al. Copper as Dietary Supplement for Bone Metabolism: A Review. Nutrients. 2021;13(7):2246.
38. Huang T, Yan G, Guan M. Zinc Homeostasis in Bone: Zinc Transporters and Bone Diseases. Int J Mol Sci. 2020;21(4):1236.
39. Fleming DE, Ware CS. Portable x-ray fluorescence for the analysis of chromium in nail and nail clippings. Appl Radiat Isot. 2017;121:91–5.
40. Wittry DB, Barbi NC. X-ray Crystal Spectrometers and Monochromators in Microanalysis. Microsc Microanal. 2001;7(2):124–41.
41. Doubly curved crystals direct x-rays [Internet]. [cited 2023 Nov 7]. Available from: https://spie.org/news/doubly-curved-crystals-direct-x-rays
42. Specht AJ, Obrycki JF, Mazumdar M, Weisskopf MG. Feasibility of Lead Exposure Assessment in Blood Spots using Energy-Dispersive X-ray Fluorescence. Environ Sci Technol. 2021;55(8):5050–5.
43. Nie H, Chettle D, Luo L, O'Meara J. Dosimetry study for a new in vivo X-ray fluorescence (XRF) bone lead measurement system. 2007;263:225–30.
44. Specht AJ, Weisskopf MG, Nie LH. Theoretical modeling of a portable x-ray tube based KXRF system to measure lead in bone. Physiol Meas. 2017;38(3):575–85.
45. Low-Level Cumulative Lead and Resistant Hypertension: A Prospective Study of Men Participating in the Veterans Affairs Normative Aging Study | Journal of the American Heart Association [Internet]. [cited 2022 Jan 31]. Available from: https://www.ahajournals.org/doi/https://doi.org/10.1161/JAHA.118.010014.
46. Grashow R, Sparrow D, Hu H, Weisskopf MG. Cumulative lead exposure is associated with reduced olfactory recognition performance in elderly men: The Normative Aging Study. Neurotoxicology. 2015;49:158–64.
47. Hu H, Aro A, Payton M, Korrick S, Sparrow D, Weiss ST, et al. The relationship of bone and blood lead to hypertension. The Normative Aging Study JAMA. 1996;275(15):1171–6.
48. Shih RA, Hu H, Weisskopf MG, Schwartz BS. Cumulative lead dose and cognitive function in adults: a review of studies that measured both blood lead and bone lead. Env Health Perspect. 2007;115(3):483–92.
49. Gherase MR, Al-Hamdani S. Improvements and reproducibility of an optimal grazing-incidence position method to L-shell x-ray fluorescence measurements of lead in bone and soft tissue phantoms. Biomed Phys Eng Express. 2018;4(6): 065024.
50. Gherase MR, Al-Hamdani S. A microbeam grazing-incidence approach to L-shell x-ray fluorescence measurements of lead concentration in bone and soft tissue phantoms. Physiol Meas. 2018;39(3): 035007.
51. Hauptman M, Niles JK, Gudin J, Kaufman HW. Individual- and Community-Level Factors Associated With Detectable and Elevated Blood Lead Levels in US Children: Results From a National Clinical Laboratory. JAMA Pediatr. 2021;175(12):1252–60.
52. Wang X, Mukherjee B, Park SK. Does Information on Blood Heavy Metals Improve Cardiovascular Mortality Prediction? J Am Heart Assoc. 2019;8(21): e013571.
53. Ruiz-Hernandez A, Navas-Acien A, Pastor-Barriuso R, Crainiceanu CM, Redon J, Guallar E, et al. Declining exposures to lead and cadmium contribute to explaining the reduction of cardiovascular mortality in the US population, 1988–2004. Int J Epidemiol. 2017;46(6):1903–12.
54. Xu T, Lin K, Cao M, Miao X, Guo H, Rui D, et al. Patterns of global burden of 13 diseases attributable to lead exposure, 1990–2019. BMC Public Health. 2023;23(1):1121.
55. United States. Agency for Toxic Substances and Disease Registry. Toxicological profile for lead [Internet]. Atlanta, Ga.: U.S. Dept. of Health and Human Services, Public Health Service, Agency for Toxic Substances and Disease Registry,; 2007. 1 online resource (528 p.). Available from: http://purl.fdlp.gov/GPO/gpo31474. Accessed 13 Nov 2023.
56. Hoover C, Dickerson AS, Specht AJ, Hoover GG. Firearm-related lead exposure and pediatric lead levels in Massachusetts: A decade of evidence (2010–2019). Environ Res. 2023Jun;15(227): 115719.
57. Hoover C, Hoover GG, Specht AJ. Firearm licenses associated with elevated pediatric blood lead levels in Massachusetts. Environ Res. 2021;1(202): 111642.